Electrochimica Acta, Vol. 27, No. 1, pp. 1–7, 1982.
Printed in Great Britain.

0013–4686/82/010001–07 $03.00/0

THE POTENTIODYNAMIC FORMATION AND REDUCTION OF A SILVER SULFIDE MONOLAYER ON A SILVER ELECTRODE IN AQUEOUS SULFIDE SOLUTIONS

VIOLA I. BIRSS

Chemistry Department, University of Ottawa, Ottawa, Ontario, K1N 9B4 Canada

and

GRAHAM A. WRIGHT

Chemistry Department, University of Auckland, Auckland, New Zealand

(*Received 5 January 1981*)

Abstract—A potentiodynamic study of silver electrodes in aqueous sulfide solutions, carried out to form phase silver sulfide films, revealed that a monolayer of silver sulfide forms as a distinct and separate stage of film growth at an underpotential of about 0.12 V. The monolayer peak (and its cathodic counterpart) was also characterized by a linear relationship between peak current density and potential sweep rate and a constant charge density of about 0.2 mC/cm^2. The potentiodynamic E/i curves for the silver sulfide monolayer were simulated by computer on the basis of a mechanism of the initial adsorption of HS^- on the silver surface in a fast equilibrium step followed by a rate determining electron transfer step to form AgHS as a surface intermediate. The AgHS species then rapidly diffuses on the surface and joins a growing two-dimensional silver sulfide monolayer nucleus. Under the experimental conditions studied here, the formation and reduction of the silver sulfide monolayer was found to be of intermediate kinetic reversibility.

INTRODUCTION

In the preceding paper[1], the kinetics and mechanism of the growth of anodic silver sulfide films on Ag in aqueous sulfide solutions was studied by the potentiodynamic method. In that paper, it was shown that prior to the onset of phase Ag_2S film formation by

$$2Ag + HS^- + OH^- \rightleftharpoons Ag_2S_{(film)} + H_2O + 2e \quad (1)$$

at the reversible potential, E_r,

$$E_r = -684 - 29.5 \log (HS^-)\,(OH^-)\ \text{mV} \quad (2)$$

a small pre-peak was observed on the potentiodynamic potential/current (E/i) curves at an underpotential, η, of about 120 mV, where

$$\eta = E_{pa} - E_r \quad (3)$$

and where E_{pa} is the potential at the peak of the anodic pre-peak.

It is the purpose of this paper to show that this pre-peak represents a unique and distinct stage of anodic silver sulfide film growth, namely that of a single and complete *monolayer* of Ag_2S on the Ag electrode surface. Also, the mechanism of the formation and reduction of the Ag_2S monolayer will be described.

Prior to this work, there have been many reported cases of the adsorption of monolayers of organic compounds, such as methanol, CO, and various dyes[2–8] on metal surfaces. Also, there are numerous examples of the deposition of metals as a monolayer on other metal substrates. These often are found to deposit at an underpotential (*upd*), depending on the difference in the values of the work functions of the two metals[9]. For example, the deposition of Tl on Ag is seen by two successive monolayer peaks, both occurring at an underpotential[10]. Similarly, the deposition of a monolayer of Pb on single crystals of Ag occurs in the *upd* manner[11]. In other work, monolayers of Ag and Cu on Pt substrates have been detected by X-ray photoelectron spectroscopy[12]. These metal deposits were shown to occur as a two-dimensional atomic array rather than as a metallic cluster.

Noble metal oxides are frequently known to form initially as monolayers as is seen, for example, in the potentiodynamic curves of Pt[13]. E/i curves of Au also clearly show the deposition of a monolayer of Au oxide at an underpotential, as do Ru and Ir[14]. Cu oxide is also found to deposit initially in two sub-monolayer stages by a random electrodeposition mechanism[15].

To date, there have been no reports in the literature of the electrochemical formation of monolayers of metal sulfides on metal electrodes in aqueous solutions although the formation of metal sulfide monolayers should be as likely as the formation of metal oxide monolayers. In particular, the tendency towards silver sulfide monolayer formation is shown in work carried out on the adsorption of sulfur on silver from the gas phase. A study of the room temperature reaction between Ag and S vapor by field emission spectroscopy[16] showed that initially, a two-dimensional Ag sulfide layer forms with a high silver/sulfur bond energy of -89 kJ/mol. This comparatively strong binding energy of sulfur to silver, which would support a complete coverage of silver by sulfur before

further Ag_2S film would form, is also seen by the fact that once sulfur is adsorbed on Ag, sulfur will hardly re-dissolve despite the concurrent field evaporation of Ag[17].

In the work presented in this paper, a smooth Ag rotating disc electrode (*rde*) was polarized potentiodynamically in aqueous sulfide solutions and the observed Ag_2S pre-peak was studied for the dependence of its charge and current densities on the potential sweep rate (s), the electrode rotation rate (ω) and the HS^- concentration. The E/i curves of the pre-peak were then simulated by computer on the basis of various models of monolayer growth and a mechanism of Ag_2S monolayer growth was determined on the basis of a best-fit approach.

EXPERIMENTAL

Cyclic potentiodynamic experiments were carried out as described previously[1] with a *rde* consisting of a Ag rod (Engelhardt, 5N purity, apparent area 0.386 cm^2) embedded in a PVC holder. Although the reference electrode was a saturated calomel electrode in a Luggin capillary, all potentials are given with respect to the normal hydrogen electrode (*nhe*) scale. The mechanical and electrochemical pretreatment of the Ag electrode surface was carried out as described previously[1]. The roughness factor, γ, equal to the ratio of the true to the apparent surface area, was obtained by double layer capacitance measurements[18] prior to the addition of sulfide to the cell.

The sulfide solution was made up as described previously[1] and all chemicals used and all conditions of experimentation were also identical to those described previously[1]. Aliquots of the stock sulfide solution were added to the cell after the precycling of the potential was complete and while the potential of the electrode was held negative of the potential for phase Ag_2S formation. The potential was also kept negative of the potential for phase Ag_2S formation during the study of the pre-peak in order to prevent the large increases in surface area observed after phase Ag_2S was formed and reduced[1].

In some experiments, the shape of the cathodic portion of the pre-peak was significantly distorted by the occurrence of the hydrogen evolution reaction (*her*) in this potential range. In the worst cases, both the anodic and the cathodic peaks of the monolayer were actually superimposed on the cathodic *her* currents. The degree of interference between the *her* and the Ag_2S monolayer formation and reduction reactions varied between experiments, probably due to variations in the condition of the electrode surface. The results reported in this paper are for experiments in which the *her* occurred at potentials sufficiently negative to avoid overlap with and distortion of the monolayer peaks.

RESULTS

Under all conditions studied, the Ag_2S pre-peak could be detected at the foot of the main anodic peak of the potentiodynamic E/i curve for Ag in aqueous sulfide solutions (Fig. 1). The pre-peak occurred at an

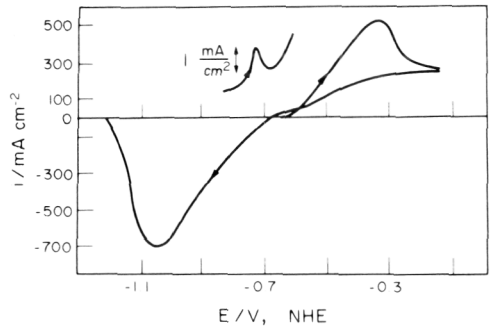

Fig. 1. E/i curve for phase Ag_2S formation and reduction on a Ag electrode in 0.5 mol/l HS^- + 0.5 mol/l NaOH solution at s = 50 mV/s and ω = 15 Hz. The Ag_2S monolayer can be detected at a high sensitivity current scale at an underpotential of about 120 mV relative to phase Ag_2S film formation.

underpotential of about 0.12 V from the reversible potential for Ag_2S formation [equation (2)]. Figure 1 shows that the current scale for the pre-peak is much smaller than that for the main anodic and cathodic peaks for phase Ag_2S formation and reduction and indicates that a much smaller amount of film forms in the pre-peak than in the main peaks.

As discussed in the previous paper[1], a complete cycle of potential carried out as in Fig. 1 results in the formation of a rather thick Ag_2S film in the anodic scan which subsequently reduces in the cathodic scan to form a very rough and porous Ag deposit of uncertain surface area. Because of these area uncertainties with complete cycles of potential, the Ag_2S pre-peak was studied by keeping the potential negative of that for phase Ag_2S formation and thereby preventing phase Ag_2S film growth.

In the study of the pre-peak, each experiment was commenced by cycling the potential of the Ag disc electrode in a sulfide-free NaOH solution (Fig. 2, dashed line). In this range of potential, only a charging current was observed from which the true electrode area could be determined by double layer capacitance measurements. Then, a specified amount of sulfide was added to the cell and the anodic pre-peak and its

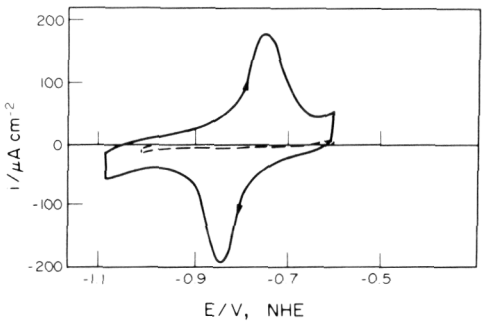

Fig. 2. Comparison of E/i curve of Ag in 2 mol/l NaOH solution prior to HS^- addition (– – –) and in 3.2 mol/l HS^- + 2 mol/l NaOH solution (——) at s = 100 mV/s shows the Ag_2S pre-peak in a potential range negative of phase Ag_2S film formation.

cathodic counterpart developed immediately (Fig. 2, solid line). The size and the shape of the pre-peaks were found to be stable with time of potential cycling which indicates that the peaks cannot be related to the presence of impurities in the solution, which would be anticipated to build up with time on the electrode surface. Also, the pre-peak remained stable and unchanged despite an extension of the potential negatively into the range of hydrogen evolution or an extension somewhat positively where phase Ag_2S growth commenced (Fig. 3). When the potential was extended still more positively, much more phase Ag_2S film was formed and then the reduction of the Ag_2S monolayer became obliterated by the large cathodic peak of phase Ag_2S reduction. With larger amounts of phase Ag_2S growth, the surface area of the electrode began to increase with each complete cycle of potential and the magnitude of the pre-peak was seen to also increase with increasing electrode area.

The characteristics of the Ag_2S pre-peak have been studied by determining the dependence of its charge density, current densities and peak potentials on the HS^- concentration (ranging from 3 to 100 mmol/l), s and ω. The results reported here are typical for those experiments in which the Ag_2S monolayer peaks were clearly separated from the current due to the *her*.

(i) *Effect of* ω

Under all conditions studied, the E/i trace of the pre-peak is independent of ω which indicates that mass transport in solution is not a rate limiting step in the oxidation and reduction processes occurring in the pre-peak. This lack of influence of ω also confirms the fact that solution impurities are not involved in the reactions of the pre-peak.

(ii) *Dependence of charge densities on* s *and* HS^- *concentration*

Under all conditions studied, the charge density in the pre-peak remained constant at 0.20 ± 0.01 mC/cm^2. This observed charge density can be compared to a theoretical calculation of the anticipated charge density, q_m, of a uni-molecular layer of Ag_2S on the silver surface. The structure of the Ag_2S monolayer is estimated from an electron diffraction study of the epitaxial growth of thin Ag_2S layers (35 nm) on Ag in aqueous sulfide solutions[19]. Despite a wide variety of Ag crystal planes which were exposed to the aqueous sulfide solution, Ag_2S was found to form only with its $(0\bar{1}2)$ plane parallel to the Ag surface. The $(0\bar{1}2)$ plane of Ag_2S (which has a monoclinic structure[20]) consists of sulfur atoms arranged at the corners of parallelograms having sides 0.423 nm in length. From this structure, a density of 5.2 g/cm^3 for the Ag_2S monolayer can be deduced and a theoretical charge density of 0.18 mC/cm^2 is obtained. The closeness of the observed and the calculated charge densities supports the contention that the pre-peak represents the formation of an Ag_2S monolayer prior to phase Ag_2S film growth.

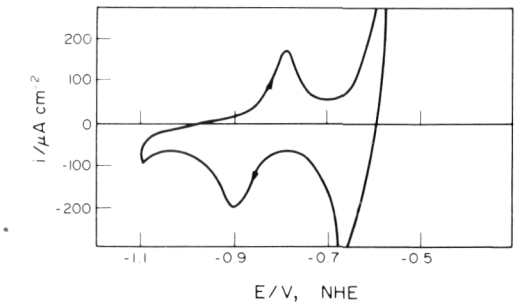

Fig. 3. Extension of the potential of the Ag electrode into the potential range in which phase Ag_2S film forms in 95 mmol/l $HS^- + 2$ mol/l NaOH solution at $s = 100$ mV/s shows that phase Ag_2S film reduces separately from the reduction of the Ag_2S monolayer.

(iii) *Effect of* s *and* HS^- *concentration on current densities and peak potentials*

Under all conditions studied, the relationship between the peak *cd* and s was found to be linear (Fig. 4). A linear relationship such as this, rather than a linear $i/s^{1/2}$ relationship as is found for thicker film formation (phase Ag_2S growth[1]), is indicative of a surface reaction and in particular, of monolayer formation and reduction[13, 21–24]. This linear i_p/s relationship can be predicted for the spreading of a layer across an electrode surface when θ, the degree of surface coverage, depends on the applied potential, E

$$i = q_m \frac{d\theta}{dt} = q_m s \frac{d\theta}{dE}. \quad (4)$$

In this work, θ at the anodic and cathodic peaks was found to be equal to approximately 0.55 under all conditions.

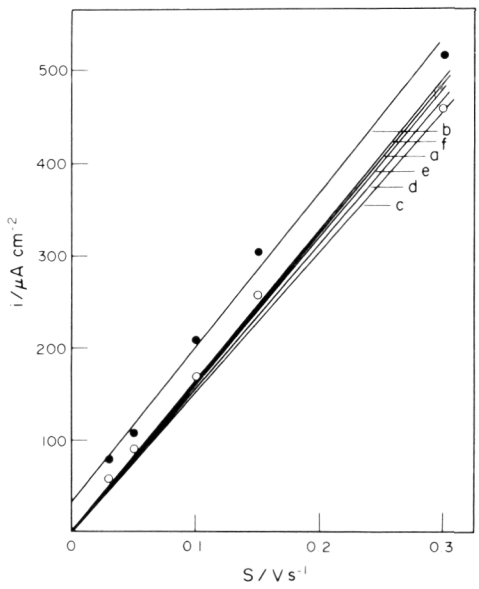

Fig. 4. *Experimentally observed* relationship between peak current density for (a) Ag_2S formation (o) and (b) reduction (•) and s for HS^- concentrations ranging between 3 and 100 mmol/l. *Calculated* relationship between peak current densities and s for HS^- concentrations of (c) 3.2, (d) 9.4, (e) 39, (f) 95 mmol/l by equation (13) for the mechanism of Ag_2S monolayer formation and reduction as given by reactions (5–7).

Figure 4 also shows that a change in the HS^- concentration by a factor of about 30 has only a minor effect on the observed peak cd; this indicates once again that the rate of the reaction in the pre-peak is not controlled by a solution diffusion step. From the slope of the i_p/s plot in Fig. 4, a peak capacitance of 1.7 mF/cm^2 was obtained for the Ag_2S monolayer reaction.

At all s and HS^- concentrations, η remained constant at 120 ± 5 mV and the peak width at half height, $E_{1/2}$, also remained approximately constant at a value of about 90 mV. However, the anodic and cathodic peak separation, ΔE_p, was found to increase from about 80 mV at $s = 30$ mV/s to about 120 mV at $s = 300$ mV/s as the degree of irreversibility of the E/i trace increased.

MECHANISM OF Ag_2S MONOLAYER FORMATION AND REDUCTION

In order to determine the mechanism of Ag_2S monolayer growth on the Ag anode, the experimentally obtained potentiodynamic E/i curves have been simulated by computer on the basis of several proposed mechanisms of monolayer growth. The selected mechanism was chosen on the basis of the best fit between the experimental and the calculated E/i curves. As a unimolecular layer has a simply geometry uncomplicated by the unknown structure and morphology of thicker films, it is quite possible to deduce the mechanism of its growth by a curve simulation method and from this, obtain valid kinetic information.

The following simple mechanism for the anodic formation of a silver sulfide monolayer has been deduced and the corresponding kinetic equations used for the curve simulations are given below.

Initially, it is considered that HS^- adsorbs on the Ag surface in a fast equilibrium adsorption step as in reaction (5), producing the adsorbed intermediate, $Ag(HS^-)_{ads}$. This is considered to be the most abundant surface intermediate

$$\underset{(1-\theta-\theta')}{Ag} + \underset{c_{HS^-}}{HS^-} \overset{K_1}{\rightleftharpoons} \underset{\theta'}{Ag(HS^-)_{ads}}. \quad (5)$$

A Langmuir isotherm is used to describe the surface adsorption, with the equilibrium constant, K_1, being independent of the potential. It is assumed that the diffusion of HS^- to the Ag surface is fast in comparison with the rate of the adsorption step (5), as is supported experimentally. The magnitude of the double layer charging current is small in comparison with the anodic and the cathodic peak currents and therefore can be ignored.

Reaction (5) is followed by a slow, rate determining charge transfer step (6) which is activation controlled

$$\underset{\theta'}{Ag(HS^-)_{ads}} \underset{k_{-2}}{\overset{k_2}{\rightleftharpoons}} \underset{\theta''}{AgSH} + e^-. \quad (6)$$

The surface concentration of AgSH, θ'', is assumed to be very small. AgSH is known as a soluble compound[25] and so is a realistic choice as a surface intermediate. Analogously, NiHS has been postulated as a surface intermediate in the pitting of Ni surfaces in HS^- solutions[26].

The electron transfer step (6) is followed by the rapid diffusion of AgSH along the Ag surface to a nucleation site, perhaps one of the growing two-dimensional nuclei of the final monolayer product. Then AgSH reacts with an OH^- species in a fast equilibrium step (7) to form the product while releasing water

$$\underset{\theta''}{-R\text{—}AgSH} + \underset{c_{OH^-}}{OH^-} \overset{K_3}{\rightleftharpoons} \underset{\theta}{-R\text{—}Ag\text{–}S\text{–}} + H_2O. \quad (7)$$

Using a Langmuir isotherm, the fraction of the Ag surface which is covered by the growing R–Ag–S– nuclei [reaction (7)] can be denoted by θ, while $(1-\theta-\theta')$ denotes the fraction of free Ag surface.

The Faradaic current for reaction (6) can be expressed as

$$i = zFk_2\theta' \exp\left(-\frac{\beta zFE}{RT}\right) - zFk_{-2}\theta'' \times \exp\left[-\frac{(1-\beta)zFE}{RT}\right] \quad (8)$$

where $z(=1)$ is the number of electrons transferred in reaction (6) and k_2 and k_{-2} are the forward and the reverse rate constants for reaction (6) when the applied potential is zero. β, the transfer coefficient, is assumed to be 0.5. θ' can then be expressed in terms of equilibrium (5)

$$K_1 = \frac{\theta'}{(1-\theta-\theta')c_{HS^-}}. \quad (9)$$

Equation (9) can be rearranged to yield

$$\theta' = \frac{K_1 c_{HS^-}(1-\theta)}{1+K_1 c_{HS^-}}. \quad (10)$$

K_3 from reaction (7) can be expressed as

$$K_3 = \frac{\theta}{\theta'' c_{OH^-}} \quad (11)$$

which gives

$$\theta'' = \frac{\theta}{K_3 c_{OH^-}}. \quad (12)$$

Equation (8) can now be re-written as

$$i = \frac{Fk_2 K_1 c_{HS^-}(1-\theta)}{1+K_1 c_{HS^-}} \exp\left(\frac{FE}{2RT}\right) - \frac{Fk_{-2}\theta \exp(-FE/2RT)}{K_3 c_{OH^-}}. \quad (13)$$

Equation (13) can be solved numerically for cd as a function of potential. The parameter, A, defined in equation (14) and B, in equation (15), are obtained by computer and then K_1 and k_2 are obtained separately.

$$A = \frac{Fk_2 K_1 c_{HS^-}}{1+K_1 c_{HS^-}} \quad (14)$$

$$B = \frac{Fk_{-2}}{K_3 c_{OH^-}}. \quad (15)$$

K_3 and k_2 cannot be obtained separately without experimentally changing the concentration of OH^-.

In the calculation, E_1, the starting potential, was obtained from the experimental E/i curves as the potential at the onset of the anodic current in the pre-peak (−1.00 V). θ_0, the initial fraction of the covered Ag surface was given a small but finite value of 0.001. A, containing the constants K_1 and k_2, and B, were selected by trial and error during the curve simulation.

$$K_1 = 1.7 \times 10^2 \text{ l/mol}$$
$$k_2 = 2.84 \times 10^{-2} \text{ mol/cm}^2\text{ s}$$
$$B = 3.0 \times 10^{-8} \text{ mA/cm}^2.$$

In each iteration of the calculation, t was incremented by $\Delta t = 0.01$ s, E was incremented by $\Delta E = s\Delta t$ and θ was incremented by $\Delta\theta = i\Delta t/q_m$. In this manner, both the anodic and cathodic curves of the pre-peak were calculated at all s and HS^- concentrations studied experimentally.

Several of the experimental and calculated E/i curves are shown for $s = 100$ mV/s in Fig. 5 and it can be seen that the fit is quite good over the entire range of HS^- concentrations studied. Qualitatively, Fig. 5 shows that the experimental i/E curves tend to be somewhat narrower at half-height than the calculated ones.

This probably indicates that attractive forces exist between the molecules of the Ag_2S monolayer[27] as was suggested for Ag_2S in a study of the chemisorption of S on Ag from a H_2S/H_2 mixture[28]. The effect of attractive forces within the layer is to make the curves narrower and somewhat higher[27] while repulsive forces within the layer would have the opposite effect. The fit between the calculated and experimentally obtained curves at various s can be seen in Fig. 4, where lines c–f represent the calculated i_p/s relationship over the entire range of HS^- concentrations and the points (lines a and b) are the experimentally obtained data.

Nevertheless, the mechanism of a simple one-electron transfer reaction, preceded by the adsorption of HS^- on the Ag surface and followed by a fast, two-dimensional film growth step results in calculated E/i curves which are a very good match with the experimentally observed curves. This mechanism seems to hold over the entire range of s and HS^- concentrations studied here.

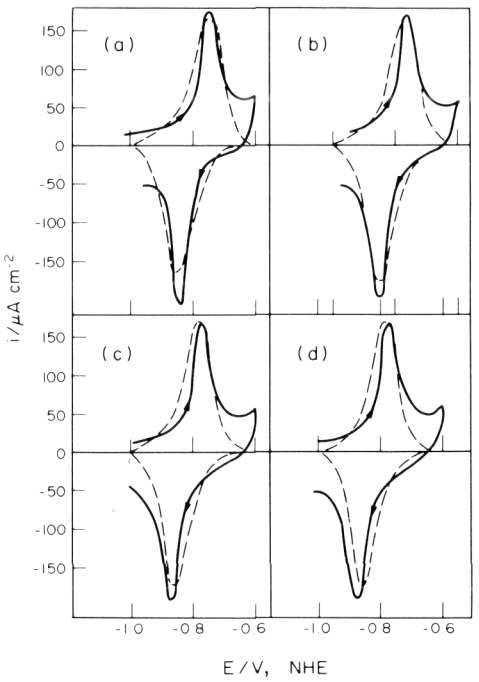

Fig. 5. Comparison of the experimentally observed (——) and the calculated (– – –) [equation (13)] E/i curves for Ag_2S monolayer formation and reduction in aqueous sulfide solutions of (a) 3.2, (b) 9.4, (c) 39, (d) 95 mmol/l HS^- + 2 mol/l NaOH at 100 mV/s.

OTHER POSSIBLE MECHANISMS

(i) *Simultaneous two-electron transfer mechanism*

An alternative mechanism for the formation and reduction of the Ag_2S monolayer is that of a simultaneous two-electron transfer step rather than a one-electron transfer step as outlined above. This would invoke the bridging of the HS^- between two neighbouring Ag atoms. However, it is not very likely that two electrons would simultaneously cross an identical energy barrier. Also, the computer simulated E/i curves based on this type of mechanism are much narrower and sharper than those for the one-electron transfer mechanism and the fit is particularly poor at higher HS^- concentrations. For these reasons, the simultaneous two-electron transfer mechanism for Ag_2S monolayer formation has been rejected.

(ii) *Consecutive two electron transfer mechanism*

A second alternative mechanism for the Ag_2S monolayer formation reaction invokes the transfer of two electrons in two separate steps as in reactions (16)–(18), where the latter is assumed to be the rate determining step

$$\underset{(1-\theta)}{\text{Ag}} + \underset{c_{HS^-}}{\text{HS}^-} \overset{K_4}{\rightleftharpoons} \underset{\theta'}{\text{Ag(HS}^-)_{ads}} \tag{16}$$

$$\underset{\theta'}{\text{Ag(HS}^-)} \overset{K_5}{\rightleftharpoons} \underset{\theta''}{\text{AgHS}} + e \tag{17}$$

$$\underset{(1-\theta)}{\text{Ag}} + \underset{\theta''}{\text{AgHS}} + \underset{c_{OH^-}}{\text{OH}^-} \underset{k_{-6}}{\overset{k_6}{\rightleftharpoons}} \underset{\theta}{\text{Ag}_2\text{S}} + \text{H}_2\text{O} + e \tag{18}$$

θ' and θ'' are considered to be small, AgSH is considered to be mobile on the electrode surface, and θ is the fraction of the silver surface which is covered by the final product, Ag_2S. The E/i curves for this mechanism have been calculated and the results show that the calculated anodic curves are very sharp and narrow while the cathodic ones are low and broad. If reaction (17) had been considered to be the rate determining step, the calculated anodic curve is then low and broad and the cathodic peak is sharp and narrow. Because one of the most striking features of the experimental E/i curves is the symmetrical shape of the anodic and cathodic peaks, the asymmetry of the calculated curves

invalidates the two consecutive electron transfer reaction mechanism.

KINETICS OF SILVER SULFIDE MONOLAYER FORMATION AND REDUCTION

It can be readily seen from the general appearance of the E/i curves for silver sulfide monolayer formation and reduction (Figs 1 and 5) that the rate determining step (6) is not kinetically reversible under the conditions of s studied here. This is seen by the fact that the anodic and the cathodic peaks are not mirror images of each other and that the anodic and cathodic peak potentials are not equal, as would be the case for a kinetically reversible surface reaction. Instead, it is seen that as s is increased, the process becomes somewhat more irreversible and that the peaks shift in the direction of the potential sweep, with the anodic peak potential becoming more positive and the cathodic peak potential becoming more negative. However, the reaction is also not fully kinetically irreversible, which would be characterized by a linear $E_p/\ln s$ relationship and this is also not observed (Fig. 6).

Therefore, in order to gauge the degree of kinetic reversibility of the silver sulfide monolayer reaction, under the conditions studied here, several characteristics of the Ag_2S monolayer peaks such as C_p, the peak capacitance, θ_p, the degree of surface coverage at the peak, and $E_{1/2}$ have been compared with the theoretical values which have been determined for various surface reaction mechanisms[27, 30].

The silver sulfide monolayer reaction mechanism is considered to be most similar to mechanism II[30]. For a ratio of $\log s/k_2$ of between 0 and 1, as is obtained for the silver sulfide case by computer modelling, the observed C_p of 1.7 mF/cm^2, θ_p of about 0.55 and $E_{1/2}$ of about 90 mV all indicate that the silver sulfide monolayer reaction can be considered to be of intermediate kinetic reversibility and being somewhat more irreversible than reversible in the range of s studied. It is clear that at rates of s much lower than 15 mV/s, the reaction would become kinetically fully reversible while at s about five orders of magnitude higher than this, the reaction would become fully irreversible[30]. However, this large range of s was not investigated for silver sulfide monolayer formation and reduction, primarily due to the frequent interference between the currents of the monolayer peak and the currents due to the *her*.

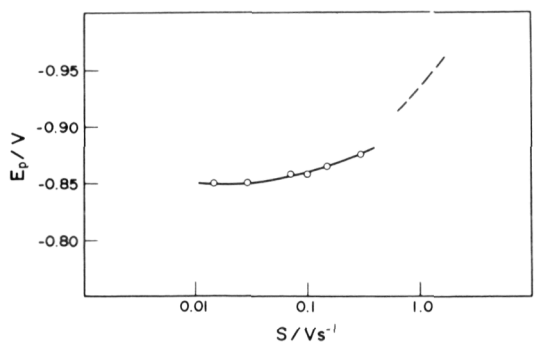

Fig. 6. Cathodic peak potential as a function of s in 9.4mmol/l HS^- + 2 mol/l NaOH solution. Fully irreversible reaction (– – –) would have slope of 120 mV while fully reversible reaction would be independent of s.

SUMMARY

A potentiodynamic study of Ag in aqueous sulfide solutions has shown that a monolayer of silver sulfide forms as a separate stage of film growth prior to the growth of a phase silver sulfide film. Under all conditions studied, the Ag_2S monolayer forms at an underpotential of about 0.120 V and has a charge density of about 0.2 mC/cm^2. The relationship between the peak currents and s is linear and the curves are independent of the electrode rotation rate. The reduction of the silver sulfide monolayer also occurs in a current peak separate from phase Ag_2S film reduction and has the same characteristics as does the anodic monolayer peak.

The E/i curves of the Ag_2S monolayer have been simulated by computer on the basis of several mechanisms of monolayer formation and reduction. The best fit between the experimental and the calculated E/i curves occurs for a mechanism involving the initially rapid adsorption of HS^- on the silver surface followed by a rate determining one electron transfer step to form AgHS, which then diffuses and reacts at a growing two-dimensional nucleation site on the Ag surface. Under the experimental conditions studied here, the Ag_2S monolayer reaction is of intermediate kinetic reversibility, having characteristics between those of a fully reversible and a fully irreversible surface reaction.

Acknowledgements—V.I.B. gratefully acknowledges the receipt of a Commonwealth Scholarship from Canada to New Zealand from the New Zealand University Grants Committee.

REFERENCES

1. V. I. Birss and G. A. Wright, *Electrochim. Acta* **26,** 1809 (1981).
2. M. W. Breiter and S. Gilman, *J. electrochem. Soc.* **109,** 622 (1962).
3. S. Gilman, *J. phys. Chem.* **67,** 78 (1963).
4. C. McCallum and D. Pletcher, *J. electroanal. Chem.* **70,** 277 (1976).
5. A. M. Mirri and P. Favero, *Ric. Sci.* **28,** 2307 (1958).
6. W. Kemula, Z. Kublik and A. Axt, *Roczniki Chem.* **35,** 1009 (1961).
7. A. M. Hartley and G. S. Wilson, *Anal. Chem.* **38,** 681 (1966).
8. M. Fujihiri and T. Osa, *J. Am. chem. Soc.* **98,** 7850 (1976).
9. R. R. Adzic and A. R. Despic, *J. chem. Phys.* **61,** 3482 (1974).
10. A. Bewick and B. Thomas, *J. electroanal. Chem.* **65,** 911(1975).
11. A. Bewick and B. Thomas, *J. electroanal. Chem.* **84,** 127 (1977).
12. J. S. Hammond and N. Winograd, *J. electroanal. Chem.* **80,** 123 (1977).

13. J. O. Zerbino, N. R. de Tacconi, A. Calandra and A. Arvia, *J. electrochem. Soc.* **124,** 475 (1977).
14. H. Angerstein-Kozlowska, B. E. Conway, B. Barnett and J. Mozota, *J. electroanal. Chem.* **100,** 417 (1979).
15. J. M. M. Droog, C. A. Alderliesten, P. T. Alderliesten and G. A. Bootsma, *J. electroanal. Chem.* **111,** 61 (1980).
16. K. Hayek and J. H. Block, *Ber. Bunsen. Ges. Phys. Chem.* **81,** 256 (1977).
17. R. Rousseau and N. Barbouth, *C. R. Acad. Sci. C.* **277,** 357 (1973).
18. M. Babai, T. Tshernikovskii and E. Gileadi, *J. electrochem. Soc.* **119,** 1018 (1972).
19. B. Rivolta, M. Lazzari and L. Bicelli, *Gazz. Chim. Ital.* **104,** 179 (1974).
20. A. J. Frueh Jr., *Z. fuer Kristallogr.* **110,** 136 (1958).
21. E. Laviron, *Bull. Soc. Chim. Fr.* **10,** 3717 (1967).
22. H. Angerstein-Kozlowska, B. Macdougall and B. Conway, *J. electroanal. Chem.* **39,** 287 (1972).
23. D. Astley, J. A. Harrison and H. R. Thirsk, *J. electroanal. Chem.* **19,** 325 (1968).
24. A. C. Ng, Ph.D. Thesis, University of Auckland (1975).
25. W. Freyberger and P. de Bruyn, *J. phys. Chem.* **61,** 586 (1957).
26. M. Kesten, *Corrosion* **32,** 94 (1976).
27. H. Angerstein-Kozlowska, J. Klinger and B. Conway, *J. electroanal. Chem.* **75,** 45 (1977).
28. J. Benard, J. Oudar and F. Cabane-Brouty, *Surface Sci.* **3,** 359 (1965).
29. S. Srinivasan and E. Gileadi, *Electrochim. Acta* **11,** 321 (1966).
30. H. Angerstein-Kozlowska, J. Klinger and B. Conway, *J. electroanal. Chem.* **75,** 61 (1977).